DECEMBER 1986 LRP 288/86

PASSIVE STABILIZATION OF AXISYMMETRIC MODES IN AN ELONGATED TOKAMAK

F. Hofmann, A.D. Turnbull and F.B. Marcus

PASSIVE STABILIZATION OF AXISYMMETRIC MODES IN AN ELONGATED TOKAMAK

F. Hofmann, A.D. Turnbull and F.B. Marcus

Centre de Recherches en Physique des Plasmas
Association Euratom - Confédération Suisse
Ecole Polytechnique Fédérale de Lausanne
21, av. des Bains - 1007 Lausanne/Switzerland

ABSTRACT

Growth rates of axisymmetric modes of elongated tokamak plasmas, in presence of a conducting shell, have been computed and the effects of plasma-wall distance, current profile and elongation have been analyzed. For highly elongated plasmas, it is found that the side walls are more important than the top and bottom walls for stabilizing these modes. Furthermore it is shown that decreasing the width of the radial current profile has a much greater effect on vertical stability than increasing the width of the conducting shell by the same amount. Finally, the conditions for axisymmetric stability during an evolution from a circular plasma to a highly elongated racetrack are investigated.

1. INTRODUCTION

Elongated tokamaks of various types have been built [1,2,3,4] and proposed [5,6]. The motivation for these projects has always been the same: an attempt to extend MHD beta limits to values which are attractive for a fusion reactor. One of the key problems inherent in these devices is the appearance of unstable axisymmetric modes. The stabilization of these modes is obviously a necessary condition for the practical feasibility of any elongated tokamak.

In this paper, we consider the passive stabilization of axisymmetric instabilies by means of a perfectly conducting shell. The analysis is performed using two numerical codes, ERATO [7] and FBT [8]. The two methods have been shown to produce essentially the same growth rates and marginal stability conditions [8], in cases which are accessible to both codes (i.e. up-down symmetric configurations). Here, we study the effects of plasma-wall distance, current profile and elongation on the vertical stability of racetrack-shaped plasmas. The influence of plasma pressure on axisymmetric modes of racetracks has previously been found to be small [8] and is not considered here. Active stabilization of elongated tokamaks, as well as effects of finite shell resistivity have been considered elsewhere [9]. Non-axisymmetric instabilities of racetrack-shaped plasmas have recently been discussed by Troyon et al. [10].

2. EFFECT OF PLASMA-WALL DISTANCE

Consider a racetrack-shaped equilibrium with elongation $\kappa = 3$. The source functions are chosen as

$$\left.\begin{aligned} p' &= c_p\,(\varphi + \ell\,\varphi^2) \\ TT' &= c_T\,(\varphi + \ell\,\varphi^2) \end{aligned}\right\} \quad (1)$$

where $\varphi = (\Psi - \Psi_{lim})/(\Psi_{ax} - \Psi_{lim})$, $c_T/c_p = R_o^2\mu_o[(1/\beta)-1]$, $\beta = 0.33$ and $\ell = -0.5$. This gives a low-β plasma ($\beta_{pol} = 0.15$) with current, pressure and q-profiles as shown in Fig. 1. We assume that the plasma is enclosed in a perfectly conducting shell as shown in Fig. 2. Using the ERATO code [7] we then compute the growth rate of the most unstable axisymmetric mode for various wall positions. In this section, we only consider up-down symmetric configurations ($D_t = D_b$). The corners of the conducting shell are rounded (Fig. 2) in order to avoid discontinuities in the vacuum equilibrium quantities in ERATO. This has only a small influence on the results. D_{si} and D_{so} are the inside and outside plasma-wall distances, measured at the height of the magnetic axis. When D_{si} and D_{so} are equal, the symbol D_s is used for both quantities.

First, we assume that the top and bottom walls are fixed and we compute the growth rate as a function of the lateral plasma-wall distance. The results are shown in Fig. 3. Here, the plasma is always centered in the shell i.e. the plasma-wall distance is the same on both sides. Note that all linear dimensions are normalized by the horizontal minor plasma radius, a. Growth rates are normalized by the Alfvén frequency, $\omega^2 = B_o^2/(\mu_o R_o^2 \rho_o)$. It is seen that, even when the top and bottom walls are far away (D_t = 2.0), the mode can still be stabilized by placing the side walls sufficiently close (D_s = 0.205). A typical mode picture close to the marginal point (D_t = 2.0, D_s = 0.208) is shown in Fig. 4. The displacement vectors are predominantly vertical but they are much larger near the magnetic axis than near the edge of the plasma, indicating that the mode pattern is far from a rigid displacement.

When the side walls are fixed and the growth rate is computed as a function of the position of the top and bottom walls, we obtain the results shown in Fig. 5. We note that, when the side walls are too far from the plasma (D_s > 0.78), the mode can no longer be stabilized, even with top and bottom walls touching the plasma surface (D_t = 0 , Fig. 6). Thus it appears that the stabilizing effect of the side walls is more important than that of the top and bottom walls. This becomes evident when we consider a typical image current distribution (Fig. 9). The induced current densities are roughly the same in all four walls. However, the current maxima in the side walls are much closer to the centre of gravity of the plasma current than the corresponding maxima in the top and bottom walls. Consequently, the side wall currents produce a larger radial field than the currents in the top and bottom walls.

Cases with asymmetric side walls are also shown in Fig. 5. It is interesting to note that the stabilizing effect of the outer wall is more important than that of the inner wall. This can again be explained with the help of Fig. 9. On the one hand, the image current density is sligthly larger on the inner wall than it is on the outer wall. On the other hand, the radial field in the centre of the plasma, produced by a unit current on the outer wall is considerably larger than the radial field produced by the same current on the inner wall. The second effect overrides the first and, hence, the outer wall is more effective for stabilization than the inner wall. Mode pictures for cases with asymmetric side walls are shown in Figs. 7 and 8. The relatively large parallel displacement at the plasma boundary in contact with the wall may be explained as follows: If we consider a typical mode pattern for a case in which none of the walls is very close to the plasma boundary (Fig. 4), we find that the predominantly vertical displacement of the central region is coupled with lateral displacements of the peripheral regions. This leads to an increase in the plasma width near the top and a corresponding decrease near the bottom. If one of the side walls is positioned very close to the plasma surface (Figs. 7 and 8), these lateral displacements are suppressed and, since the plasma behaves as an incompressible fluid, a retrograde vertical motion appears near the wall.

Figures 6, 7 and 8 also show that when one or several walls are close to the plasma boundary, the mode assumes a "convective" character. It then resembles an internal mode with relatively little displacement of the boundary. It should be noted, however, that, as far as vertical stability is concerned, there is no essential difference between the convective mode and the global mode (Fig. 4). In both cases, the centre of gravity of the plasma current is shifted vertically. This induces image currents in the walls which may or may not be able to stabilize the mode, depending on wall positions and equilibrium parameters.

3. EFFECT OF CURRENT PEAKING

It is a well-known fact that, the more the current is peaked, the more difficult it is to stabilize axisymmetric modes. Here, we are interested in the following question: given a certain amount of current peaking, what is the decrease in plasma-wall distance which is necessary in order to maintain marginal stability. Let us consider an extreme case, with elongation κ = 4 (Fig. 10). Using the same source functions as before (eq. (1)), we compute a number of equilibria with different ℓ-values and hence different current profiles. The plasma shape, the β value (β_{pol} = 0.15), and q on the edge are fixed (q_s = 2.1). Growth rates of the vertical instability are computed using the FBT code [8]. Here, the conducting shell is assumed perfectly rectangular (without rounded corners), since FBT uses (r,z) coordinates and a rectangular mesh. Cases with four different current profiles ($-0.3 > \ell > -0.6$) and several side wall positions ($0.1 < D_s < 0.5$) have been analyzed. The top and bottom walls are considered fixed ($D_t = D_b = 0.22$).

The results can be summarized in the form of a stability diagram (Fig. 11), showing the points of marginal stability in the (D_s, W) plane. W is the half width at half maximum of the radial current profile, at the height of the magnetic axis, normalized by the minor radius, a. W is a linear function of ℓ in the domain considered here. The (D_s, W) plane is then divided into stable and unstable regions by the marginal stability line (Fig. 11). The slope of the marginal stability line determines the change in plasma-wall distance (ΔD_s) which is necessary to compensate for a certain amount of current peaking (ΔW). If we define an effective lateral distance between the plasma current and the wall, $D_{eff} = 1 - W + D_S$, and assume that vertical stability is a function of D_{eff}, we would expect the slope of the marginal line to be of order unity. The fact that this slope is much less than unity may be explained as follows: A change in the radial current profile implies a simultaneous change in the vertical current profile. Therefore, when W increases, the effective plasma-wall distance is reduced everywhere. On the other hand, when D_S is reduced, only the side walls are displaced and the top and bottom walls remain fixed. In conclusion, we can state that decreasing the width of the radial current profile by a given amount is equivalent to increasing the width of the conducting shell by approximately twice that amount.

4. EFFECT OF ELONGATION AND Q-PROFILE

It has been proposed [9,11] that a highly-elongated tokamak plasma may be created by starting with a circular cross-section and then extending it until it reaches its final shape. Such a start-up scenario can be implemented in several different ways. Let us consider two cases: first, we assume that the radial current profile stays constant during the evolution. In this case, the q-profile tends to become non-monotonic and a local maximum appears on axis, at high elongation (Fig. 12). The equilibria of this sequence were generated using the source functions (1), with $\beta = 0.3$ and $\ell = -0.5$. The flux contours show that a substantial fraction of the vacuum field lines intersects the conducting wall. This has no direct influence on axisymmetric stability since the vacuum field configuration is irrelevant for ideal MHD growth rates. Nevertheless, it is often seen that unstable mode patterns exhibit large displacements perpendicular to the plasma surface mainly in those regions where the poloidal vacuum field is weak.

Growth rates of the vertical instability for the scenario of Fig. 12, as computed with FBT, are shown in Fig. 13. Here, negative values of Ω^2 indicate stable oscillations and positive values imply unstable growth. The results are shown as a function of plasma elongation, for four different side-wall positions. The fact that, in some cases, stability improves with increasing elongation (Fig. 13) may seem surprising. This is caused by the stabilizing effect of the bottom wall, which becomes effective only at high elongation. We conclude from Fig. 13 that a completely stable evolution from a circle to a $\kappa = 4$ racetrack is possible under the condition that the plasma-wall distance is approximately 25% of the horizontal minor radius.

The second scenario (Fig. 14) is characterized by a constant q-profile. In order to achieve this we need somewhat more complicated source functions, i.e.

$$\left.\begin{aligned} p' &= c_p\left[\alpha_p + \gamma_p x^{\ell} - (\alpha_p + \gamma_p)\, x^{\ell+1}\right] \\ TT' &= c_T \mu_o R_o^2\left[1 - \alpha_T x - \frac{\gamma_T}{m+1}\, x^{m+1} + \frac{\alpha_T + \gamma_T}{m+2}\, x^{m+2}\right] \end{aligned}\right\} \quad (2)$$

where
$$\gamma_p = (\ell+1)\left[\ell + 2 - \alpha_p(\ell+1)\right]$$
$$\gamma_T = (m+1)\left[m + 2 - \alpha_T(m+1)\right]$$

and
$$\chi \equiv 1 - \varphi = 1 - \frac{\psi - \psi_{lim}}{\psi_{ax} - \psi_{lim}}$$

These functions satisfy the usual boundary conditions on the edge, $p' = TT' = 0$ for $\varphi = 0$, and they produce pressure and current profiles of similar shape at low β.

The parameters used to compute the four equilibria in Fig. 14 are given in the table, below

κ	1	2	3	4
$\alpha_p = \alpha_T$	0.3	0.3	0.75	0.98
$\ell = m$	1.5	1.65	2.5	4.5
c_p/c_T	0.1	0.1	0.1	0.1

We note that the radial current profile, at the height of the magnetic axis, becomes more and more peaked as the elongation increases. Growth rates for this second scenario are shown in Fig. 15, for three different combinations of top and side wall positions. Here, vertical stability during the complete scenario requires a plasma-wall distance of approximately 0.15 a. We again observe that, for the highly-elongated plasmas ($\kappa = 3$, $\kappa = 4$), the stabilizing effect of the side walls is more important than that of the top and bottom walls. This effect has also been mentioned in a recent study by J.K. Lee [5]. It should be noted that all equilibria considered here (Fig. 14) have a very low q-value on the edge ($q_s = 2.05$). The question may therefore be asked, by how much q_s can be increased in a particular configuration, without losing vertical stability. Let us take, as an example, the $\kappa = 2$ racetrack of Fig. 14, with $D_t = D_s = 0.22$. q_s is varied by changing the parameters ℓ and m in eq. (2) within the range $0.25 < \ell, m < 1.65$, assuming $\ell = m$ and leaving all other parameters unchanged. q_o is assumed constant, $q_o = 1.05$. The growth rate of the vertical instability, as a function of q_s/q_o, is shown in Fig. 16. In this particular case, the marginal point is reached when $q_s/q_o = 4.3$.

CONCLUSION

Considering a $\kappa = 3$, low β, racetrack-shaped plasma with $q_s = 2$, we show that all axisymmetric modes can be stabilized if the plasma-wall distance is less than ~30% of the horizontal minor plasma radius. In addition, it is shown that the side walls have a greater effect on stability than the top and bottom walls. If the side walls are sufficiently close, the plasma can always be made stable, but top and bottom walls alone cannot stabilize it. If the top and bottom walls are very close to the plasma, a "convective" mode appears with relatively small perpendicular displacements on the boundary. Displacing the outer and inner walls separately, shows that the stabilizing effect of the outer wall is more important than that of the inner wall.

For the case of a $\kappa = 4$, low β racetrack-shaped plasma in a rectangular shell, the effects of current peaking and plasma-wall distance on vertical stability have been analyzed. It is shown that decreasing the width of the radial current profile by a given distance is equivalent to increasing the width of the conducting shell by approximately twice that distance.

Finally, considering a sequence of equilibria with elongation ranging from $\kappa = 1$ to $\kappa = 4$, we show that vertical stability during a complete startup evolution requires a lateral plasma-wall distance between 15 and 25% of the horizontal minor radius, the exact value depending on the assumed current profile.

ACKNOWLEDGEMENTS

Stimulating discussions with Prof. F. Troyon and Dr. S.C. Jardin are greatfully acknowledged. This work was partly supported by the Swiss National Science Foundation.

REFERENCES

[1] BORTNIKOV, A.V. at al., In Controlled Fusion and Plasma Physics (Proc. 6th Europ. Conf., Moscow, 1973), Vol. I, 165.

[2] FREEMAN, R.L. et al., In Plasma Physics and Controlled Nuclear Fusion Research (Proc. 6th Int. Conf., Berchtesgden, 1976), IAEA Vienna, Vol. I, 317.

[3] STAMBAUGH, R.D. et al., In Plasma Physics and Controlled Nuclear Fusion Research (Proc. 10th Int. Conf., London, 1984), IAEA Vienna, Vol. I, 217.

[4] OKABAYASHI, M. et al., ibid., Vol. I, 229.

[5] LEE, J.K., Nuclear Fusion 26 (1986) 955.

[6] DELUCIA, J. et al., 13th Europ. Conf. on Controlled Fusion and Plasma Heating, Schliersee, 1986.

[7] GRUBER, R. et al., Computer Phys. Commun. 21 (1981) 323.

[8] HOFMANN, F. et al., Plasma Physics and Controlled Fusion 28, (1986) 705.

[9] MARCUS, F.B. et al., Phys. Rev. Lett. 55 (1985) 2289.

[10] TROYON, F. et al., Invited paper at the 13th Europ. Conf. on Controlled Fusion and Plasma Heating, Schliersee, 1986.

[11] HOFMANN, F. et al., In Controlled Fusion and Plasma Physics (Proc. 12th Europ. Conf., Budapest, 1985), Part. I, Vol. 9F, 50.

Fig. 1: Racetrack-shaped equilibrium with elongation $\kappa = 3$, $q_s = 2.0$, $q_0 = 1.4$, $\beta_{pol} = (8\pi\int\int p ds)/(\mu_0 I^2) = 0.15$. The dotted line indicates the plasma boundary. Current and pressure profiles are taken at the height of the magnetic axis.

Fig. 2: Cross-section of elongated tokamak ($\varepsilon = 0.06\ \pi$).

Fig. 3: Growth rate of the most unstable axisymmetric mode vs. side wall position for various top and bottom wall positions (Equilibrium, see Fig. 1).

Fig. 4: Axisymmetric mode close to the marginal point. This mode corresponds to the point labelled "F4" in Fig. 3.

Fig. 5: Growth rate of the most unstable axisymmetric mode vs. top and bottom wall position for various side wall positions (Equilibrium see Fig. 1).

Fig. 6: The "convective" mode, corresponding to the point labelled "F6" in Fig. 5.

Fig. 7: Unstable axisymmetric mode with the inner (left-hand side) wall touching the plasma (Point "F7" in Fig. 5).

Fig. 8: Unstable axisymmetric mode with the outer (right-hand side) wall touching the plasma (Point "F8" in Fig. 5).

Fig. 9: Distribution of toroidal image currents in the conducting shell. Positive values are plotted outside, negative values inside the shell.

Fig. 10: Racetrack-shaped equilibrium with elongation $\kappa = 4$, $q_s = 2.1$, $\beta_{pol} = 0.15$. Dotted line = plasma boundary.

Fig. 11: Stability diagram for $\kappa = 4$ racetrack-shaped plasmas. D_s = normalized lateral plasma-wall distance, W = normalized half width of the radial current profile.

Fig. 12: Startup scenario for a highly-elongated tokamak, with constant radial current profile.

Fig. 13: Growth rate of the most unstable axisymmetric mode vs. elongation, for the scenario with constant current profile (Fig. 11).

Fig. 14: Startup scenario with constant q-profile.

Fig. 15: Growth rate of the most unstable axisymmetric mode vs. elongation, for the scenario with constant q-profile (Fig. 13).

Fig. 16: Growth rate vs. (q_s/q_o) for a $\kappa = 2$ racetrack plasma located in the upper half of the conducting shell ($D_s = D_t = 0.22$, $D_b = 4.22$).

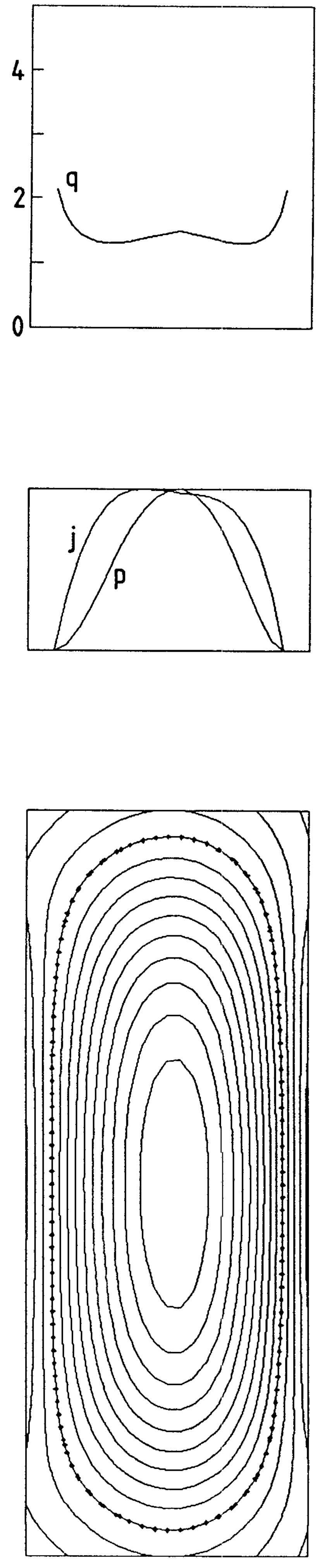

FIG.1.

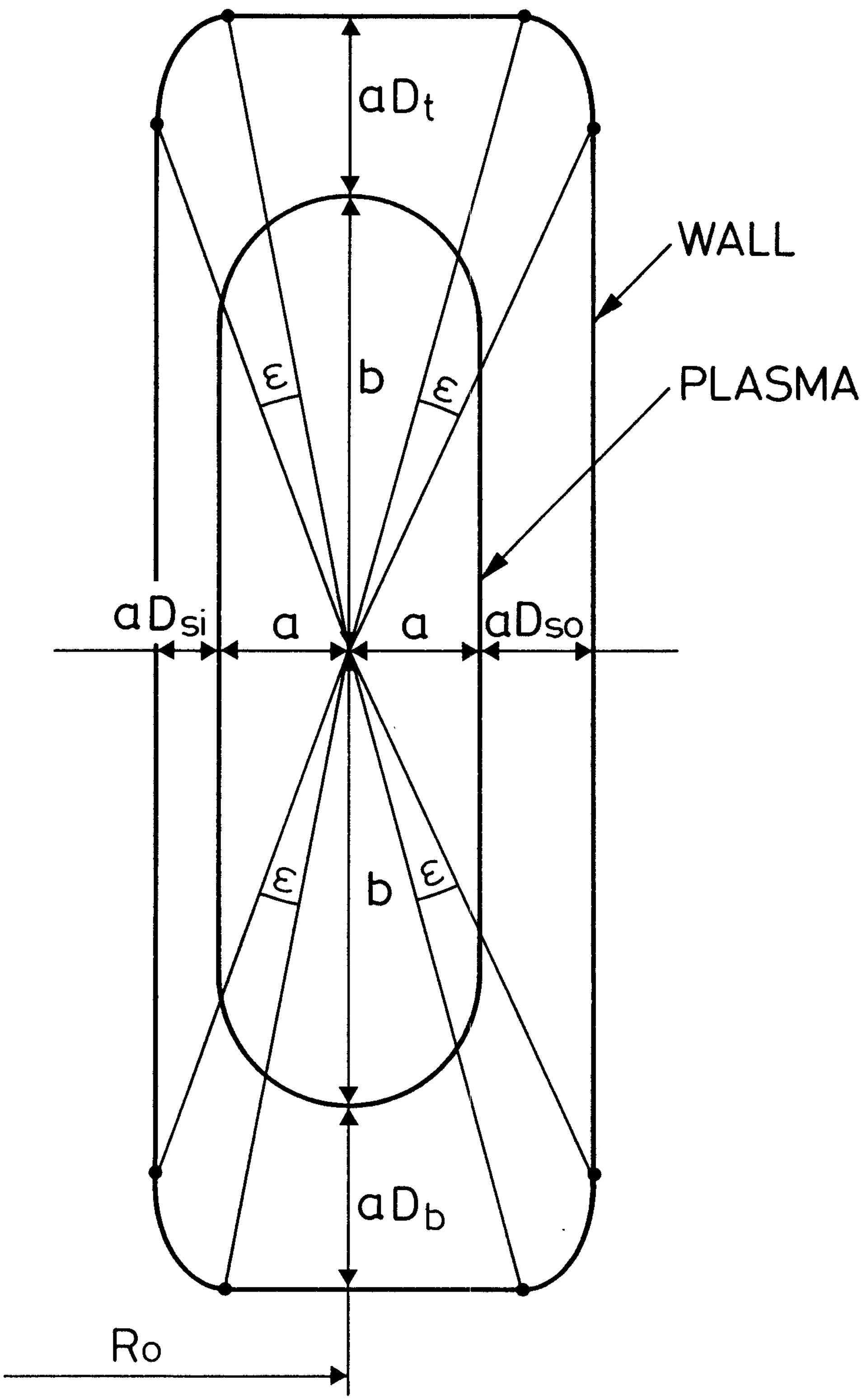

FIG.2.

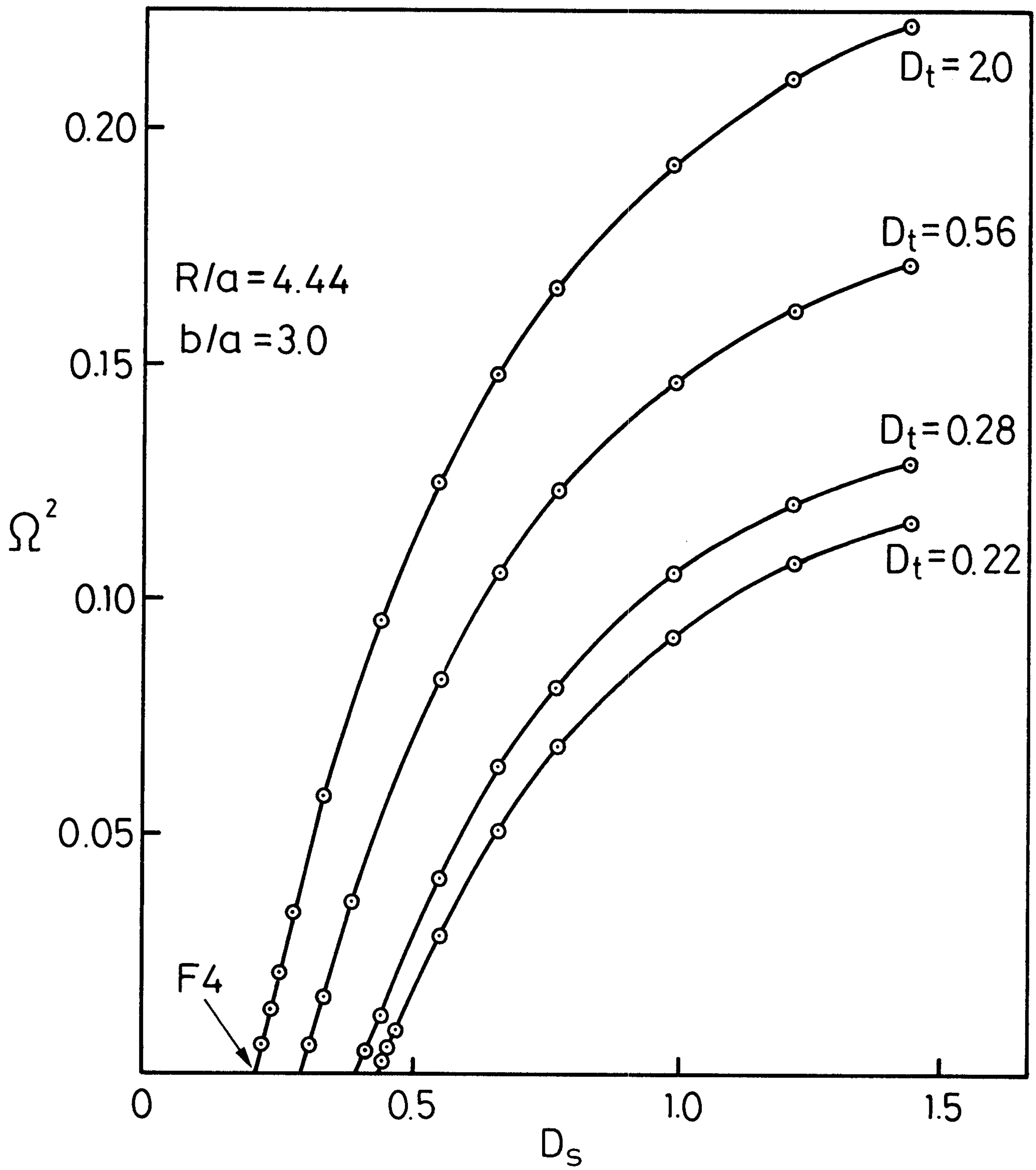

0.20
0.15
0.10
0.05
Ω^2
R/a = 4.44
b/a = 3.0
F4
$D_t = 2.0$
$D_t = 0.56$
$D_t = 0.28$
$D_t = 0.22$
0
0.5
1.0
1.5
D_s

FIG.3.

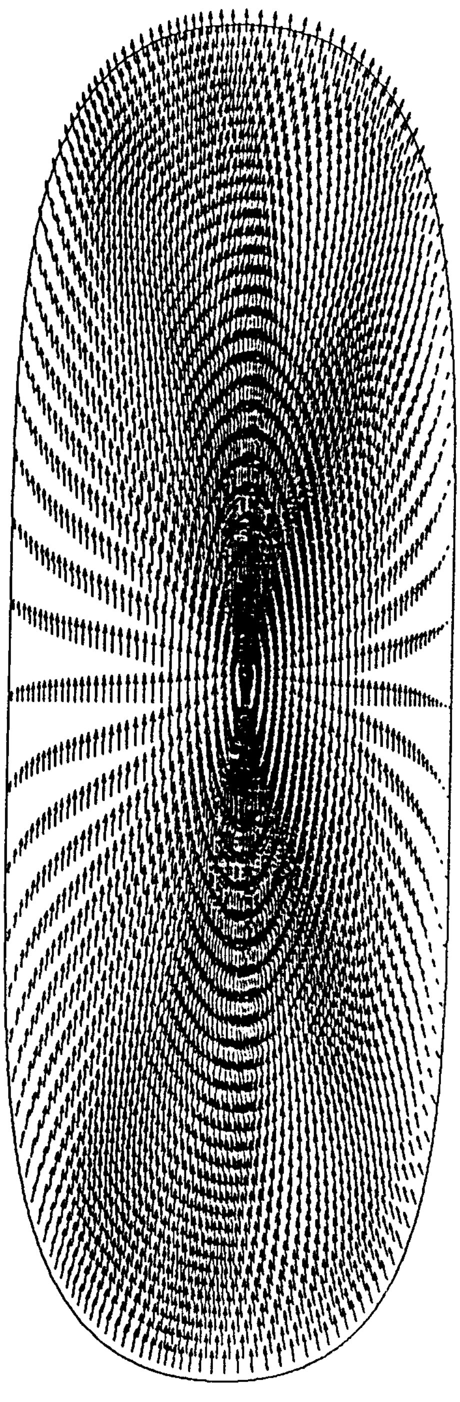

FIG.4.

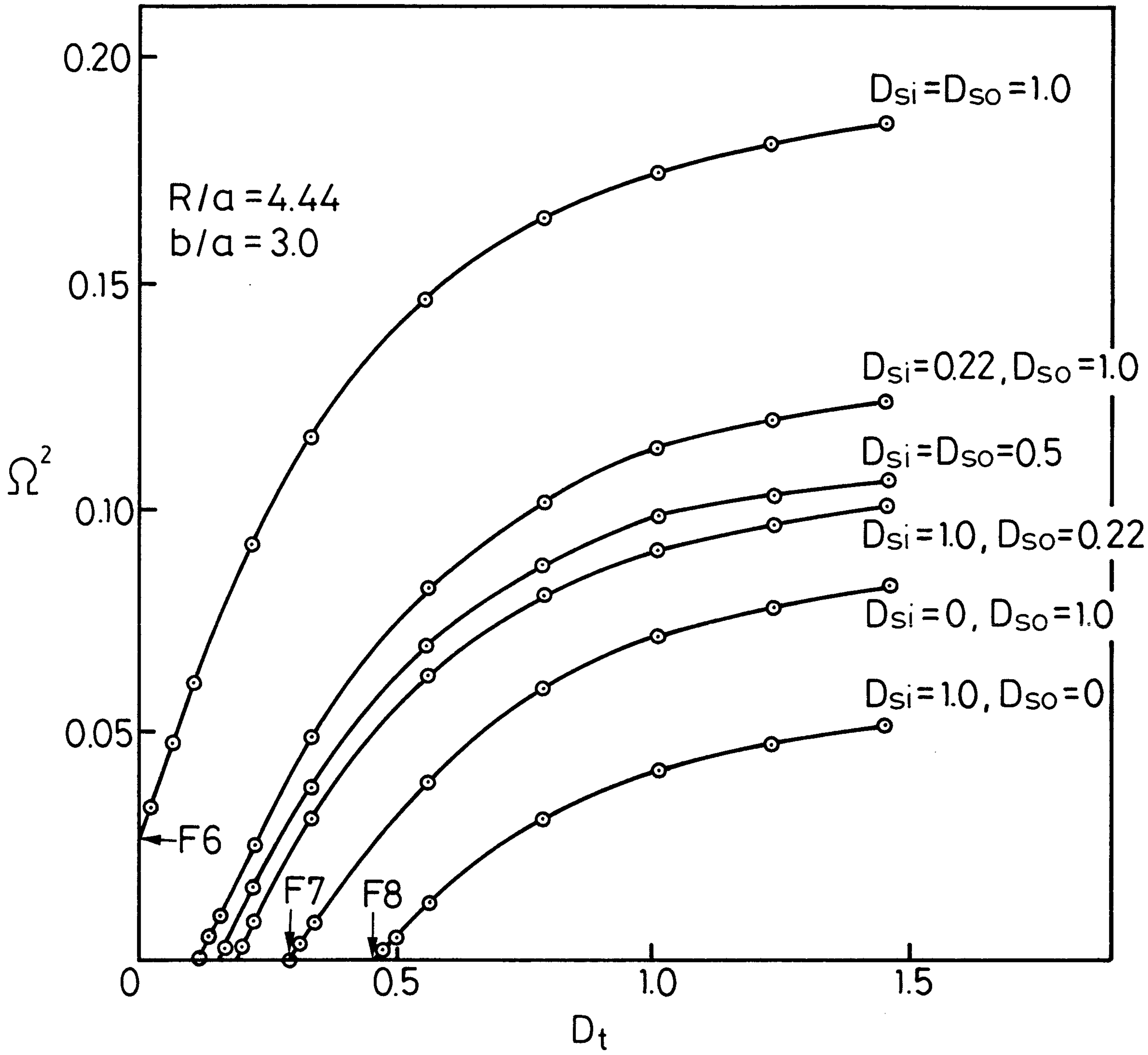

R/a = 4.44
b/a = 3.0
Dsi = Dso = 1.0
Dsi = 0.22, Dso = 1.0
Dsi = Dso = 0.5
Dsi = 1.0, Dso = 0.22
Dsi = 0, Dso = 1.0
Dsi = 1.0, Dso = 0
F6
F7
F8
0.20
0.15
0.10
0.05
0
0.5
1.0
1.5
Ω²
Dt

FIG.5.

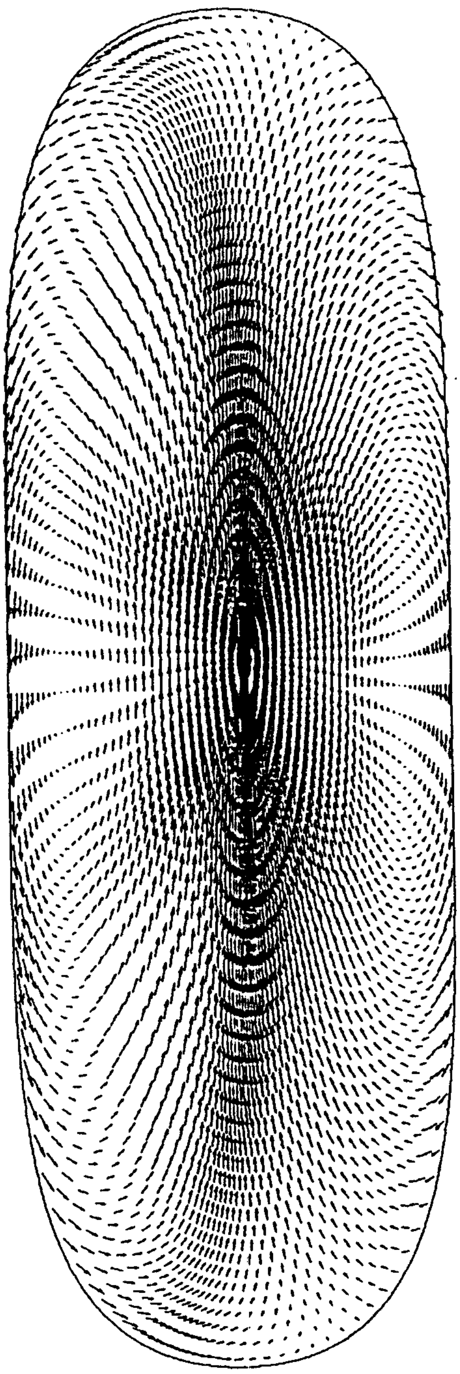

FIG.6.

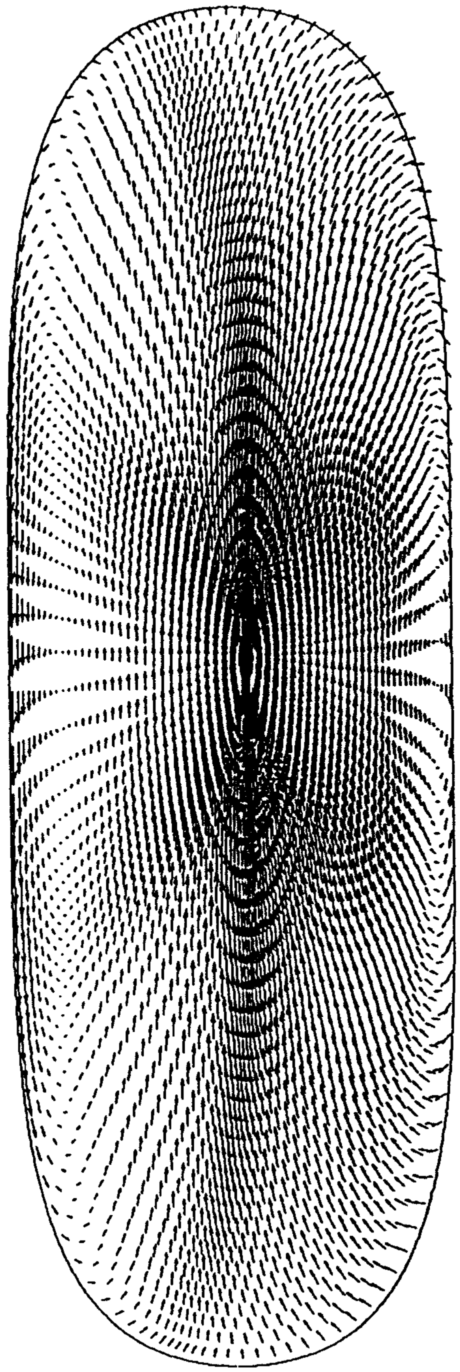

FIG.7.

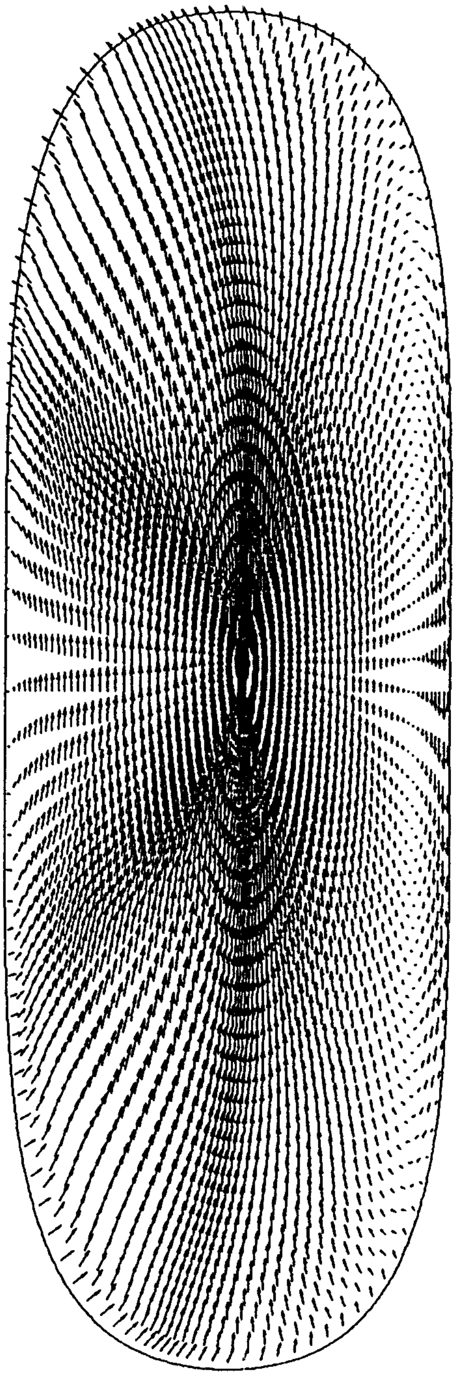

FIG.8.

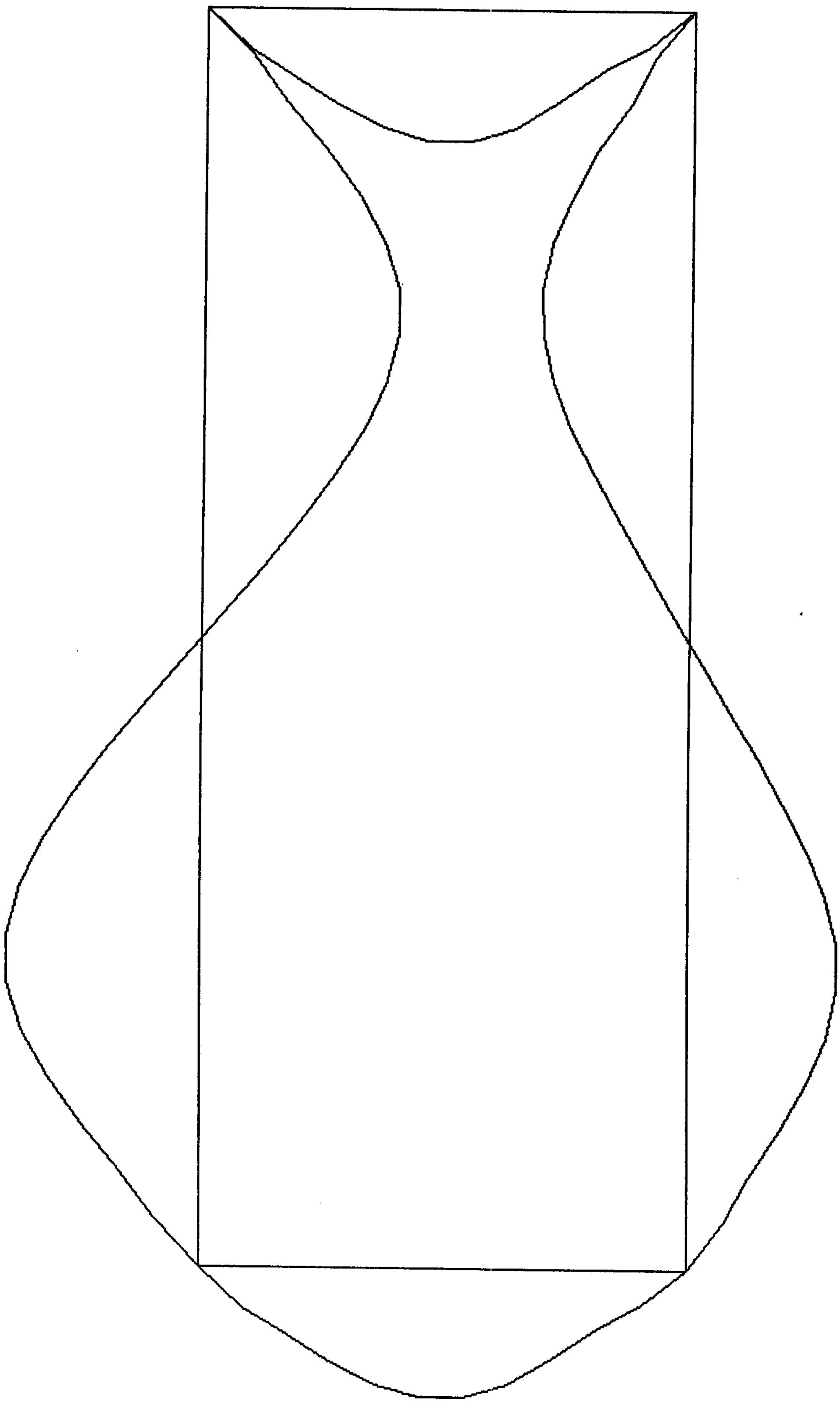

Fig. 9.

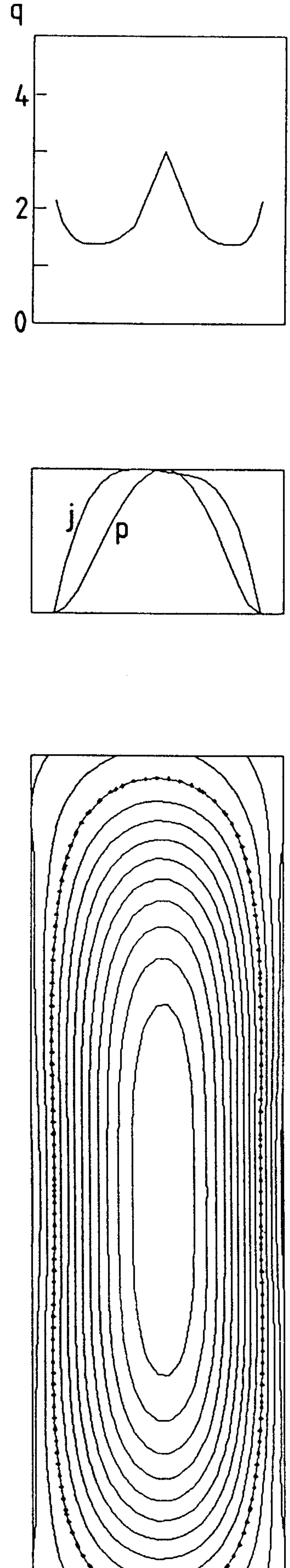

FIG. 10.

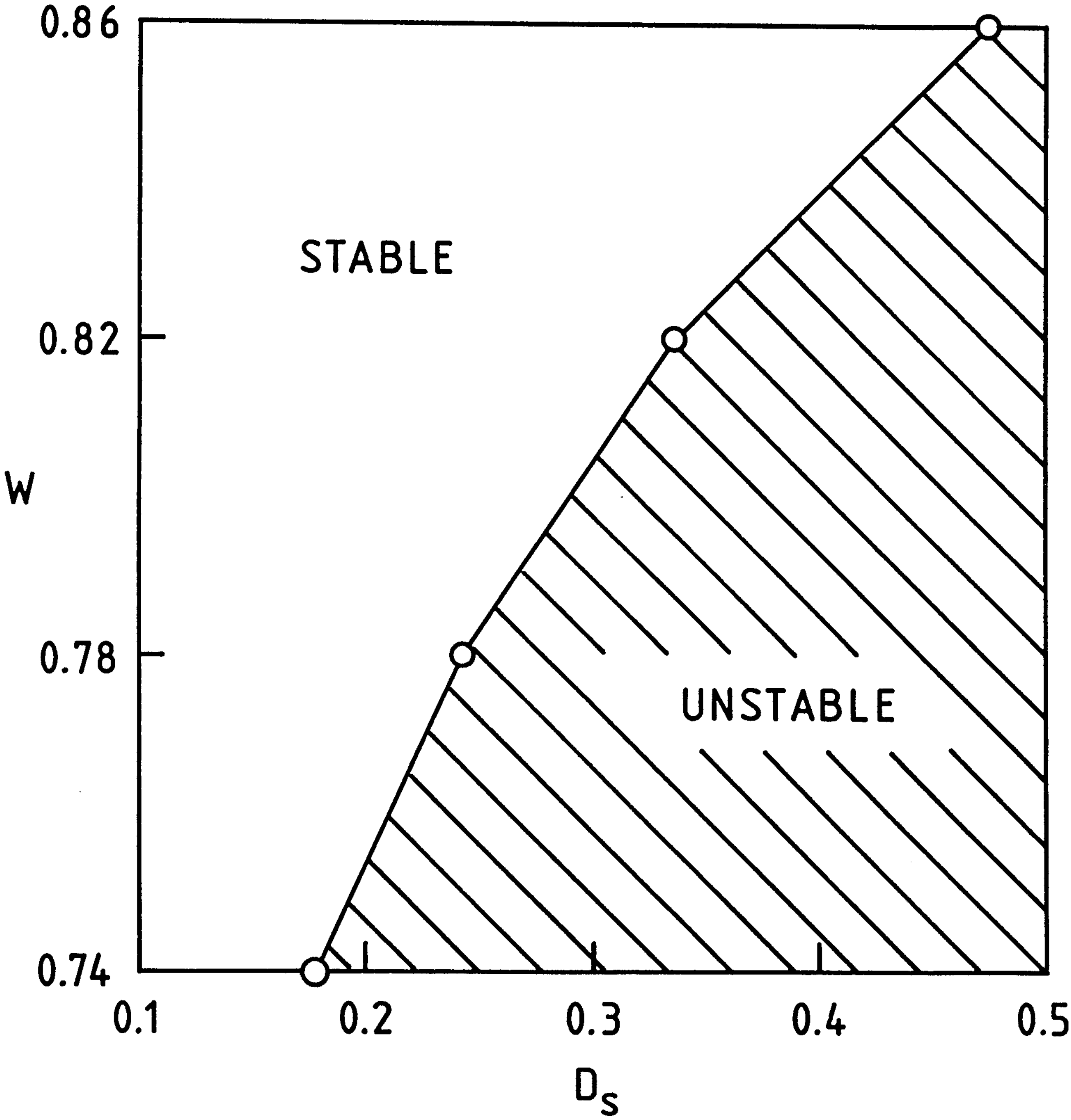

FIG. 11.

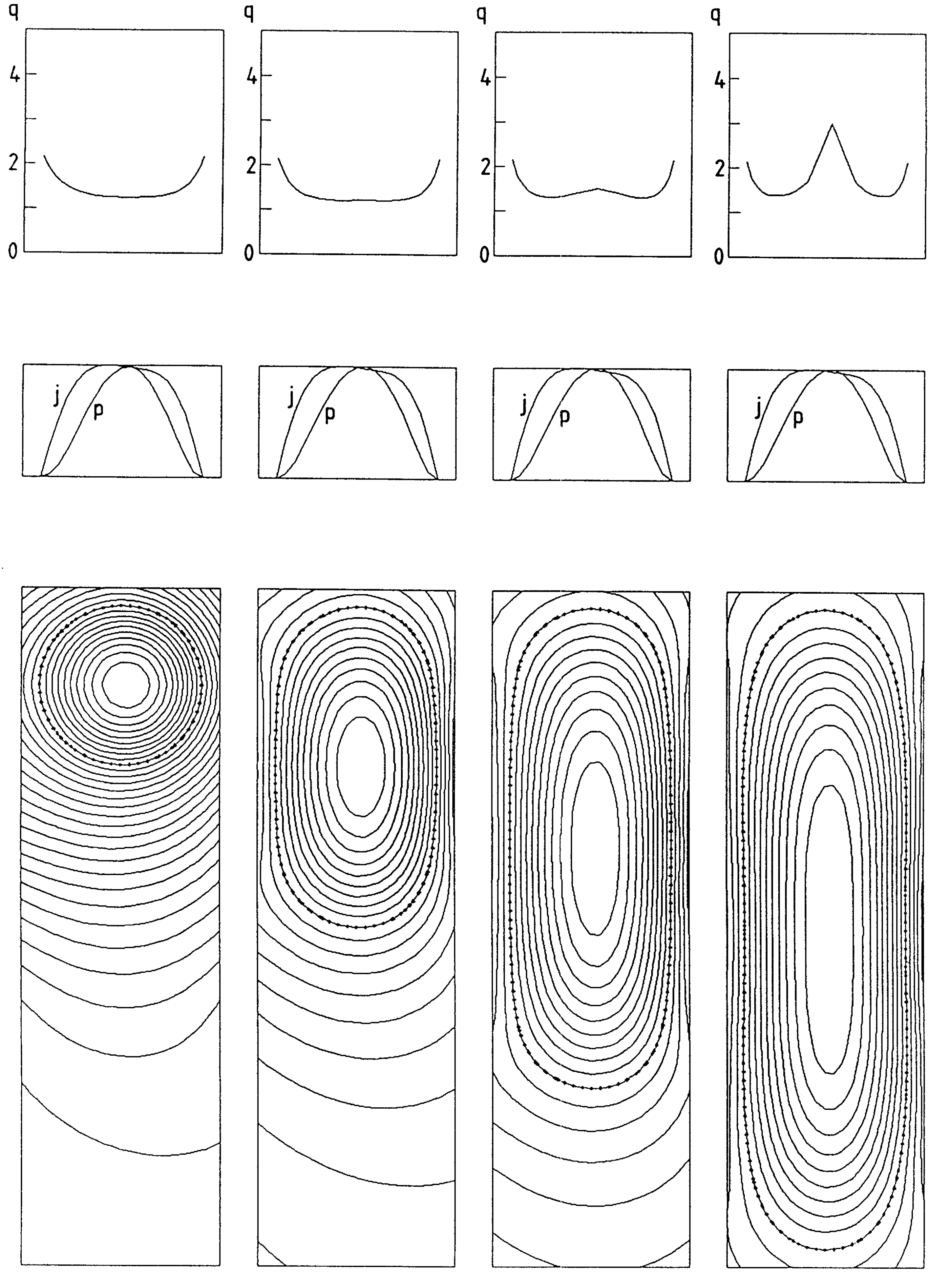

FIG. 12.

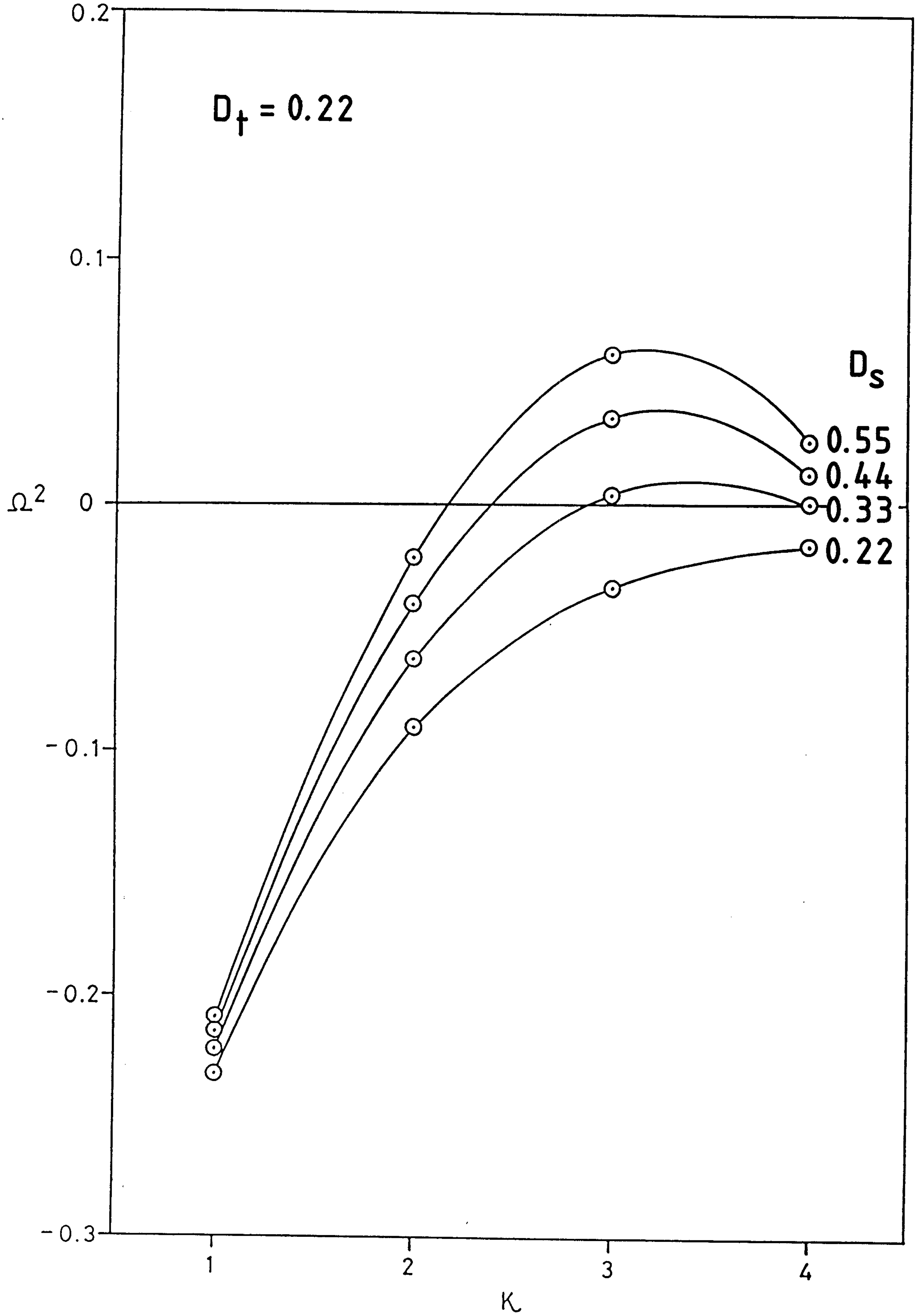

FIG. 13.

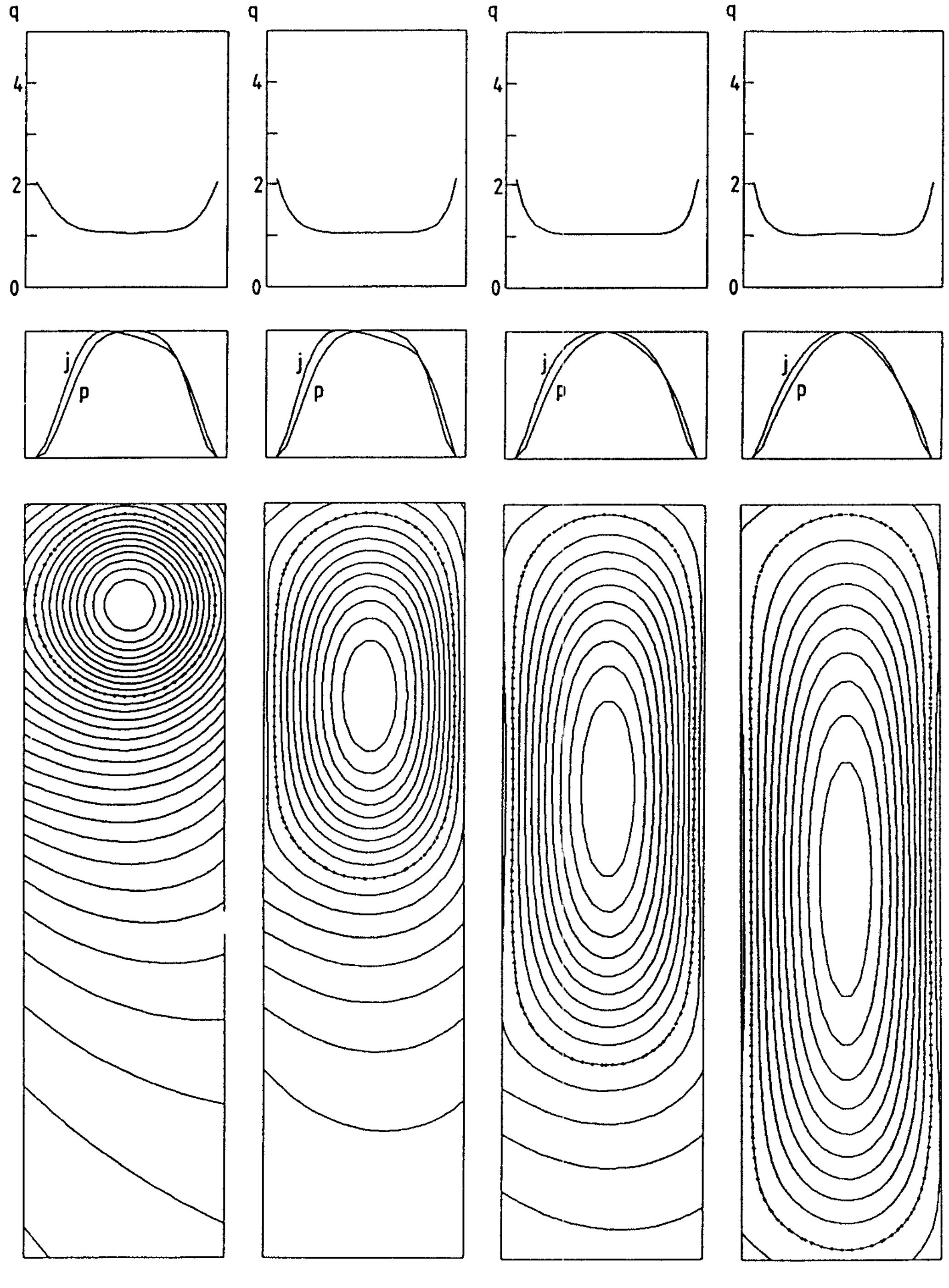

FIG. 14.

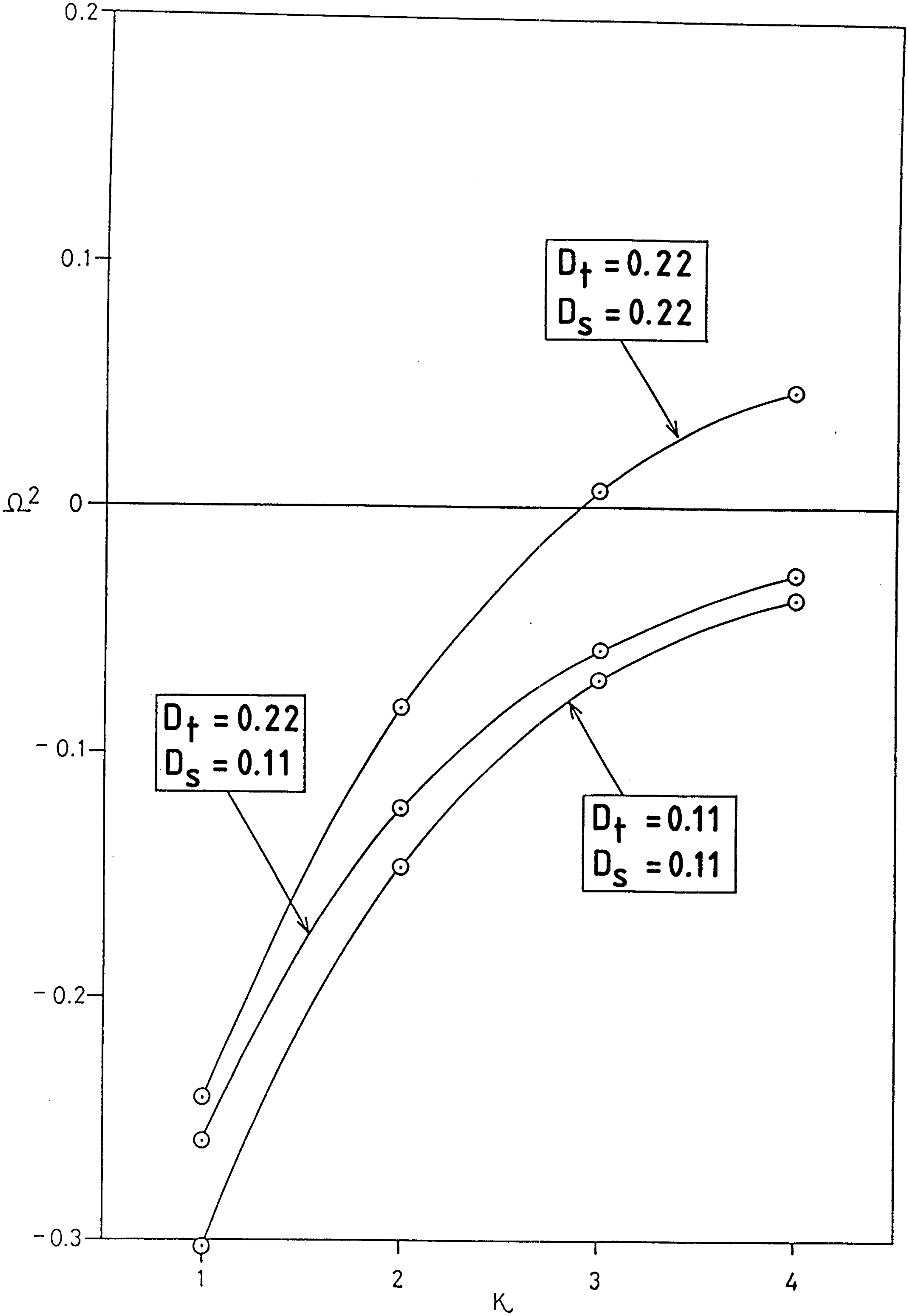
0.2
0.1
Ω^2
0
- 0.1
- 0.2
- 0.3
1
2
3
4
K
$D_t = 0.22$
$D_s = 0.22$
$D_t = 0.22$
$D_s = 0.11$
$D_t = 0.11$
$D_s = 0.11$

FIG. 15.

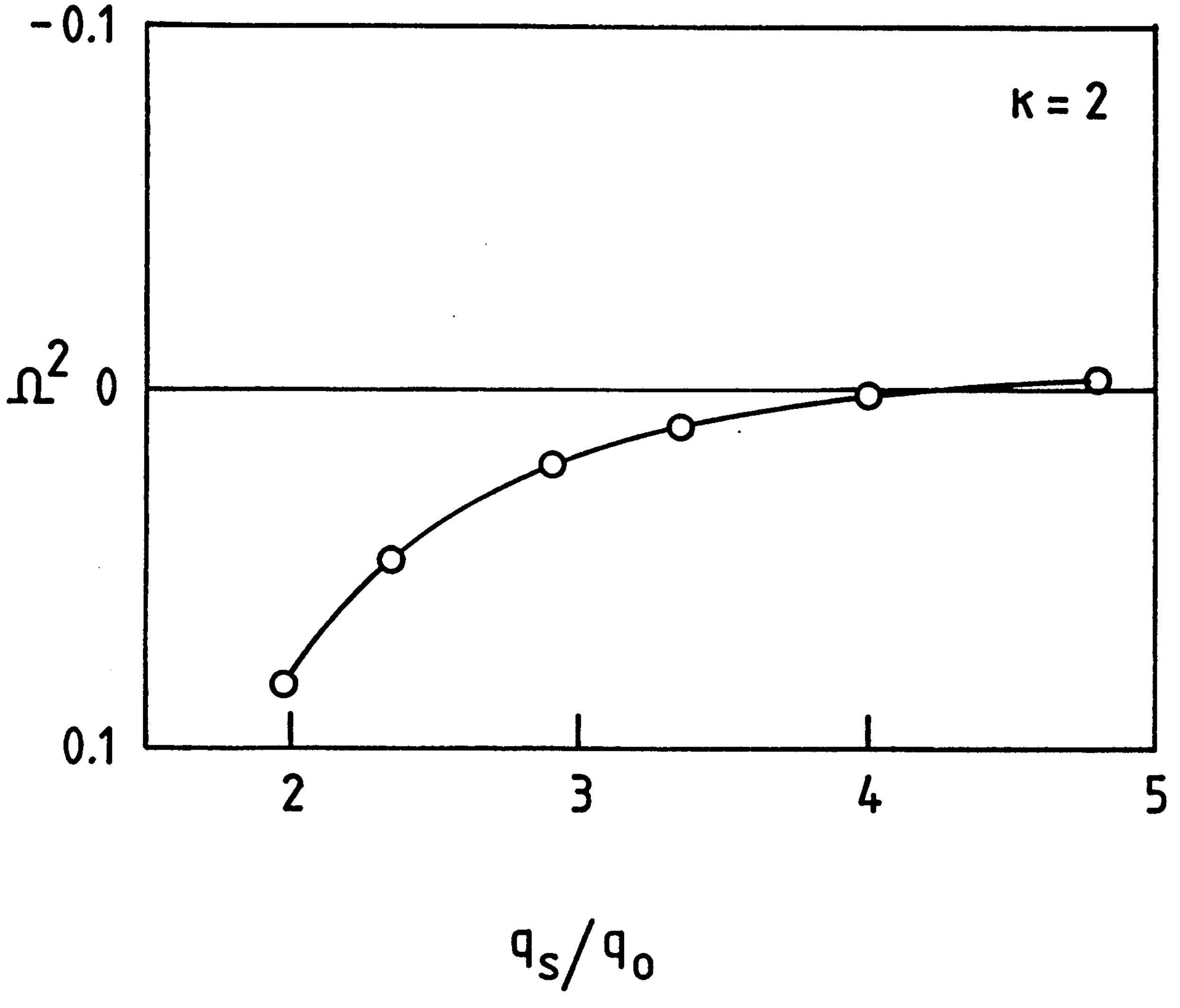

FIG. 16.